

PAPER • OPEN ACCESS

New techniques for segmentation and extraction retinal blood vessels

To cite this article: Erwin *et al* 2020 *J. Phys.: Conf. Ser.* **1500** 012090

View the [article online](#) for updates and enhancements.

You may also like

- [Multi-level spatial-temporal and attentional information deep fusion network for retinal vessel segmentation](#)
Yi Huang and Tao Deng
- [Automated Approach for Extraction of Retinal Blood Vessels](#)
Dheyaa M. Abdulsahib and Hussain F. Jaafar
- [UNet retinal blood vessel segmentation algorithm based on improved pyramid pooling method and attention mechanism](#)
Xin-Feng Du, Jie-Sheng Wang and Wei-zhen Sun



ECS
The
Electrochemical
Society
Advancing solid state &
electrochemical science & technology

DISCOVER
how sustainability
intersects with
electrochemistry & solid
state science research

New techniques for segmentation and extraction retinal blood vessels

Erwin, A Rohman, L A Nurjanah, Yurika, D Sinta, Q Al'afwa

Department of Computer Engineering, Faculty of Computer Science

Universitas Sriwijaya, Indralaya, Indonesia

erwin@unsri.ac.id, rohman020397@gmail.com, larasazrisa11@gmail.com,
yurikask15@gmail.com, dwiisinta5@gmail.com, qonitaalafwa10@gmail.com

Abstract. Blood vessels are one of the important organs in the retina that can be used to diagnose various diseases. We research blood vessel segmentation and extraction with various methods in the STARE and DRIVE dataset. The methods we use are adaptive thresholding, otsu thresholding, isodata, fuzzy c means, and bradley threshold. The parameters we use as a result of comparison are accuracy, sensitivity, and specificity. The best results of accuracy, sensitivity, and specificity in the STARE dataset were 93.66%, 92.62%, and 96.85%, respectively. The best results of the DRIVE dataset are 95.96%, 90.37%, and 98.36%, respectively.

1. Introduction

The eye is one of the senses that acts as a visual organ that interacts with light. The eye detects light and turns it into an electrochemical implus on nerve cells. The eye is the most important organ in the human body. Environmental and genetic factors can cause defects in the eye structure. As a result, visual disturbances can occur. Most eye abnormalities occur due to damage to the function of vessels in the retinal layer [1].

Blood vessels are an important part of the retina of the eye compared to other parts such as the macula, fovea, optical disc, and others. Retinal blood vessels have certain patterns and characteristics such as length, width, branching pattern, and angle [2][3][4]. treatment, and evaluation of various eye diseases [5][6].

Initially the retinal blood vessels can be marked by doctors manually, but this requires a very long time and will be a problem if given a large number of fundus images [7]. This prompted the researchers to find a way for the retinal blood vessels to be marked more easily and quickly. Therefore, automatic segmentation and extraction techniques were developed to diagnose eye disease in the retinal veins.

Retinal blood vessel segmentation provides important information for diagnosis, treatment, and evaluation of various cardiovascular and ophthalmological diseases such as hypertension, diabetes and



arteriosclerosis [8][4]. Retinal vascular extraction is also the main step to detect eye disease including diabetic retinopathy which causes blindness [9].

In segmentation and extraction retinal vessels, we propose new techniques such as adaptive thresholding, otsu thresholding, isodata, fuzzy c means (FCM), and bradley threshold combined with morphological operations, filter medians, filter morphology, etc. to get results better.

2. Related Works

Vessel segmentation and vascular extraction is one technique that can be used to diagnose diseases of the retina of the eye. Many studies have segmented blood vessels using various methods. [10] conducted a study to detect optic discs and explore tubular characteristics of blood vessels to segment veins and arteries. The method used is Wavelets Transforms and Mathematical Morphology. The results obtained by the average value of accuracy is 0.9456 but this method does not have preprocessing stages and does not have post processing. In research [11] performed blood vessel segmentation on the retinal fundus image based on the Frangi Filter and morphological reconstruction. The proposed method is evaluated using color fundus images from the DRIVE and STARE dataset. In the dataset DRIVE, the performance of the proposed method achieves an average sensitivity, specificity and accuracy of 72.13%, 96.65% and 94.50%, respectively. Whereas, on the STARE dataset it reaches an average sensitivity of 75.50%, specificity of 90.38% and accuracy of 88.76%. But in segmenting blood vessels, optical disks in retinal images are still detected.

In research [12] the attributes of retinal vessels play an important role in systemic conditions and ophthalmic diagnosis. The method used is the Extreme Learning Machine (ELM) for the retinal vessel segment. The results obtained were values of accuracy of 0.9607, sensitivity of 0.7140, and specificity of 0.9868. This method still has a lot of noise in the image of the retina, disruption of lesions, and difficulty labeling peripheral vessels. In research [13] performed blood vessel segmentation using the Human Visual System (HSV) line detection model. The proposed method was able to obtain sensitivity 73.38% and 73.84%, specificity 96.45% and 96.57%, with an average accuracy of 94.45% and 94.03% for each STARE and DRIVE database. But there is a trade-off between the detection of narrow blood vessels and there is still noise, so there is still an error in blood vessel segmentation. In research [14] segmented blood vessels using the ant colony optimization method. The study uses the DRIVE dataset and gets the accuracy of 94.5%. But in the process of blood vessel segmentation, there is still noise or white spots. In research [7] segmented with adaptive thresholding using Gauss window A common goal is for segment blood vessels by removing noise in the background.

In research [15] using the Matched filter (MF) technique with an optimized particle swarm optimization (PSO) algorithm was used to enhance images by edgels to improve filter performance. The DRIVE dataset is implemented with the concepts of MF and MF with first-order derivatives from the Gaussian (MF-FDOG). This method get an accuracy of 91.2% and a specificity of 97.2%. This method is able to improve the performance of filters to extract the structure of fine blood vessels, but there are obstacles in detecting very small vessels, vascular connectivity and low testing accuracy. In research [16] used regional and Hessian feature methods for image analysis in the diagnosis of retinal abnormalities. Using the DRIVE dataset produces a sensitivity value of 72.05% with an accuracy of 94.79%, but this proposed method cannot detect fine blood vessels. While in the research [17] can segment fine vessels with the method of Fuzzy C-Mean clustering, and local adaptive thresholding. This method is able to detect fine vessels in the image of the retina so that the fine vessels do not disappear.

In research [18] presented a new technique for segmenting retinal vessels using a phase of stretching transformation along with morphological operators to eliminate noise. The proposed method does not

show flaws segmented around the optical disk and detect the smallest vessels, because it has used phase information for detection. In addition, this technique is carried out faster segmentation, which is also important in diabetic retinopathy screening.

3. Methods

In this study, we used images from the STARE dataset and images from the DRIVE dataset. This study uses new techniques for blood vessel segmentation and extraction. The steps of segmentation and extraction in this research start from pre-processing, enhancement, extraction, segmentation, and post processing. The workflow diagram in this research can be seen in Figure.1.

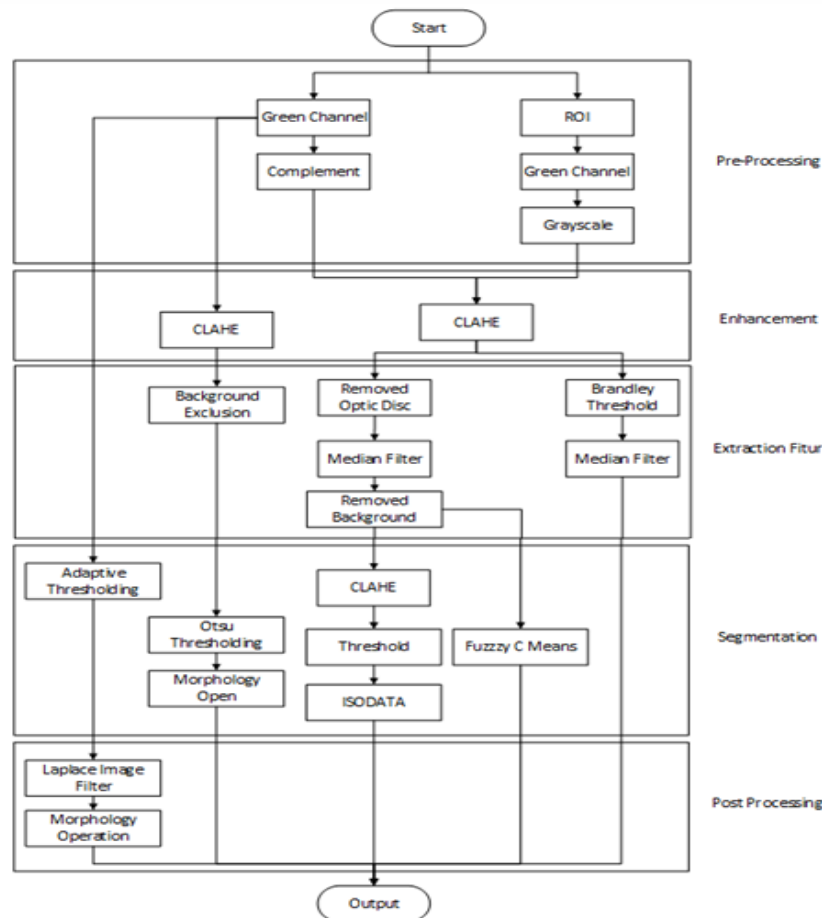


Figure 1. Diagram Block

3.1 Pre-Processing

The following are the pre-processing stages for each technique :

1. In adaptive thresholding and otsu thresholding techniques, the original image is converted to a green channel image.
2. In the ISODATA and fuzzy c means techniques, the original image is converted into a green channel image, then the green channel image is converted again into a complement image.

3. In the bradley threshold extraction technique, the first step will be the ROI Selection to select the region or part of the retinal image for processing. After that, the image of the ROI Selection will be converted into the green channel image. Then, the green channel image will be converted again into the gray scale image.

3.2 Enhancement

In this study, using *Contrast Limited Adaptive Histogram Equalization (CLAHE)* and *Laplace Filter* enhancement techniques.

3.3 Fitur Extraction

At this stage, performed optical disc removal using an *open morphology technique*, *background exclusion* and *bradley threshold*. In addition to removing optical discs, open morphology is also used in background removal operations.

3.3.1 Morphology Operation

Morphology operation is a collection of techniques used in extracting a component that serves to represent and describe areas of form such as boundaries, skeletons and convex [19]. The opening operation is generally used to break the thin line that connects two large regions and removes thin bumps. The morphological opening of set A by B is the process of erosion followed by widening the yield by B [20]. The opening operation can be seen in equation (1) as follows:

$$A \circ B = (A \ominus B) \oplus B \quad (1)$$

3.3.2 Background Exclusion

The Background Exclusion process uses Average Filter. Using *imfilter* which functions to implement the Average Filter. And use *imsubtract* which is used to add and subtract images so that the vessels can be seen.

3.3.3 Bradley Threshold

Threshold to convert fundus images into binary images. Each pixel on the image is set to black if the brightness is lower than the average brightness of the surrounding pixels [21]. The advantage of this method is that subjective images are almost as good as the Sauvola method but the calculation is twice as fast as the Sauvola method. The Sauvola method calculates local averages and local variances, while the Bradley method only calculates local averages.

3.4 Segmentation

3.4.1 Adaptive Thresholding

Adaptive thresholding is an ambition that uses a local threshold value, which is calculated adaptively based on the adjacent static pixels. Adaptive thresholding is used to convert objects consisting of gray scale pixels only in black and white pixels in scale. A pixel value of 0 represents white and a pixel value of 255 represents black with numbers from 1 to 254 representing different gray levels. The local adaptive threshold selects different threshold values for each pixel in the image based on the analysis of adjacent pixels. In this case it allows objects with various contrast levels where global threshold techniques will not work satisfactorily. Simple and fast functions include threshold intensity, local window size, median value, or average minimum and maximum values. Adaptive Thresholding technique can be seen in equation (2).

$$L(x, y) = \begin{cases} 1, & \text{if } I_E(x, y) > T(x, y) \\ 0, & \text{if } I_E(x, y) \leq T(x, y) \end{cases} \quad (2)$$

Where $L(x, y)$ is the result of Adaptive Threshold, $I_E(x, y)$ and $T(x, y)$ are representations of conditions for image enhancement and threshold functions.

3.4.2 ISODATA

The Iterative Self-Organizing Data Analysis (ISODATA) method is combining a set of procedures in a recurrent classification algorithm [22]. This process consists of cluster reunions, if the separation distance in the multispectral feature space is less than the user-specified value and instructions for separating the only cluster into two clusters [23].

The ISODATA algorithm involves the following processes :

- (1) Select the initial parameter. Different values can be assigned to these parameters and they can be modified in a repetitive process. Data points are then assigned to groups according to the parameters.
- (2) Calculate the distance index function of each cluster.
- (3) Combine or separate clusters according to the requirements given.
- (4) Repeat the iteration. Calculate the new index, and determine whether the results meet the grouping requirements. If the results are convergent, the operation ends.

The steps of this algorithm are as follows [22] :

1. Enter a dataset with points N points $\{X_i, i = 1, 2, \dots, N\}$, et the initial grouping of N_c $\{Z_1, Z_2, \dots, Z_{N_c}\}$.

No need to take the N_c value with the number of clusters. The initial value can be chosen randomly; select a value for K (Number of expected grouping centers).

Other parameters are defined as follows:

θ_n : minimum number of points that can form a cluster. A cluster will be combined with another if the number of points in it is less than θ_n .

θ_s : the maximum standard deviation of the point from the center of the cluster along each axis.

θ_c : minimum distance between two grouping centers, two clusters will join if the distance is less than θ_c .

L : the maximum number of cluster pairs that can be combined in one iteration.

I : maximum number of iterative calculations.

2. Set the dataset to the cluster.

$$\text{If } D_i = \min\{\|X_i - Z_j\|, j = 1, 2, \dots, N_c\}, \text{ then } X_i \in S_j$$

3. If the number of points in S_j is less than θ_n , leave the sample part: in the meantime, N_c minus 1.

4. Recalculate the grouping center, as in equation (3).

$$Z_j = \frac{1}{N_j} \sum_{x_i \in S_j} x_i \quad (3)$$

Where N_j is the value of S_j .

5. Let \overline{D}_j be the distance between S_j and the cluster center associated with Z_j , as in equation (4).

$$\overline{D}_j = \frac{1}{N_j} \sum_{x \in S_j} \|x - Z_j\| \quad (4)$$

6. Let \overline{D} be the overall average of this distance, as in equation (5).

$$\overline{D} = \frac{1}{N} \sum_j^N = 1 N_j \overline{D}_j \quad (5)$$

7. Determine whether division or merging is needed. If the iterative computing number has reached I , then set $\theta_c = 0$. If $N_c \leq \frac{K}{2}$, then go to step 8 and separate the cluster. For each S_j cluster, calculate vector σ_j .

8. Each σ_{ij} for the standard deviation of the coordinates from directed from Z_j to each point S_j . The standard deviation equation can be seen in equations (6) and (7).

$$\sigma_j = (\sigma_{1j}, \sigma_{2j}, \dots \dots \sigma_{nj})^T \quad (6)$$

$$\sigma_{ij} = \sqrt{\frac{1}{N_j} \sum_{k=1}^{N_j} (X_{ik} - Z_{ij})^2} \quad (7)$$

3.4.3 Fuzzy C Means (FCM)

Fuzzy c means is a data grouping technique where the existence of each data in a group is determined by the value of membership. This technique was first introduced by Jim Bezdek in 1981.

The basic concept of FCM is to determine the cluster center which will mark the average location of each cluster. In the initial conditions, the cluster center is still not accurate. Each data point has membership degrees for each cluster. By improving the cluster center and the degree of membership of each data point repeatedly, it can be seen that the cluster will move to the right location. This regulation is based on the degree of membership that describes the distance of data points given to the cluster center which is weighted by the degree of membership of the data point.

FCM calculations use the same data but are processed with a number of different clusters, so the results of the grouping will be slightly different, because the data is not processed with just one variable but with all variables. The difference in the results of grouping is because the data in a particular group is likely to move to another group if it is processed with a different number of clusters, this indicates that the application system is running correctly.

The output of the FCM is the central degree of the cluster and several degrees of membership for each data point. The FCM algorithm is structured with the following steps :

(1) Data input

Data input to be clustered is data (X) in the form of a matrix measuring $n \times m$ (n = number of data, m = attribute of each data). X_{ij} = i-data ($i = 1, 2, \dots, n$), j-attribute ($j = 1, 2, \dots, m$).

(2) Limits

Number of clusters = c

Rank = w

Maximum iteration = Maxit

Expected smallest error = ξ

Initial objective function = P_0

Initial iteration = t

(3) Generating random numbers μ_{ik} , $i = 1, 2, \dots, n$; $k = 1, 2, \dots, c$; as elements of the initial U partition matrix, with the number of each column element value in one row is 1, as in equation (8).

$$\sum_{i=1}^c \mu_{ci} = 1 \quad (8)$$

(4) Calculating the first cluster center : V_{kj} with $k = 1, 2, \dots, c$; and $j = 1, 2, \dots, m$, as in equation (9).

$$V_{kj} = \frac{\sum_{i=1}^n ((\mu_{ik})^w * X_{ij})}{\sum_{i=1}^n (\mu_{ik})^w} \quad (9)$$

(5) Calculates the objective function in the t -iteration, as in equation (10).

$$P_t = \sum_{i=1}^n \sum_{k=1}^c \left(\left| \sum_{j=1}^m (X_{ij} - V_{kj})^2 \right| (\mu_{ik})^w \right) \quad (10)$$

(6) Calculate the change in the partition matrix, as in equation (11).

$$\mu_{ik} = \frac{\left[\sum_{j=1}^m (X_{ij} - V_{kj})^2 \right]^{\frac{-1}{w-1}}}{\sum_{k=1}^c \left[\sum_{j=1}^m (X_{ij} - V_{kj})^2 \right]^{\frac{-1}{w-1}}} \quad (11)$$

with $i = 1, 2, \dots, n$; and $k = 1, 2, \dots, c$

(7) Check the stop condition :

If : $(|P_t - P_{t-1}| < \xi)$ or $(t > \text{MaxIter})$ then stop, if not : $t = t + 1$, repeat step 4 (counting V_{kj}).

3.4.4 Otsu Thresholding

Otsu is the maximum variance between clusters. The selection criteria will be obtained from the image histogram as the base and maximum variance between targets and background, this method reaches a good threshold in many cases. Assume the image is represented in the gray level $L = \{0, 1, 2, 3, \dots, L-1\}$. Taking the level of intensity from a grayscale image or from each component of an RGB image (red, green, and blue), the probability distribution of the intensity value is calculated as follows [24].

4. Result

The performance of the segmentation results is seen from the calculation of accuracy, sensitivity, and specificity. For the equation of the performance can be seen in equations (12), (13), and (14). The results of performance on images from DRIVE and images from STARE can be seen in Table 1. Comparison of the results of segmentation of each method can be seen in Table 2 and Table 3.

$$Accuracy = \frac{TP+TN}{TP+TN+FP+FN} \quad (12)$$

$$Sensitivity = \frac{TP}{TP+FN} \quad (13)$$

$$Specificity = \frac{TN}{TN+FP} \quad (14)$$

Where :

- True Positive (TP) is the number of positive data matched based on the dataset correctly.
- True Negative (TN) is the number of negative data matched based on the dataset correctly.
- False Positive (FP) is the amount of positive data but is matched based on the dataset incorrectly by the system.
- False Negative (FN) is the amount of negative data but is matched based on the dataset incorrectly by the system.

Table 1. Results of comparison of stare and drive datasets in each techniques

Research methods	STARE dataset			DRIVE dataset		
	Acc	Se	Sp	Acc	Se	Sp
Adaptive Thresholding	90.49 %	67.55%	91.77%	90.34%	62.10%	92.45%
Otsu Thresholding	89.32 %	92.62 %	89.08 %	95.96%	90.37%	96.19%
Fuzzy C Means	93.66 %	56.53%	96.66%	95.58%	73.89%	98.07%
ISODATA	89.19%	44.12%	96.85%	95.65%	67.72%	98.36%
Bradley Threshold	85.58 %	77.54 %	86.49 %	89.53%	61.97%	91.69%

In Table 1. the results of comparison of STARE dataset, it can be seen that the highest accuracy value is 93.66% using the Fuzzy C Means technique and the lowest accuracy value is 85.58% using the Bradley Threshold technique. However, the sensitivity value of the Otsu Thresholding technique is the highest sensitivity result with a result of 92.62%. Meanwhile, the lowest sensitivity value is found in the ISODATA technique with a value of 44.12%. In addition, the highest specificity value is found in the ISODATA technique with a value of 96.85% and the lowest specificity found in the Bradley Threshold technique with a value of 86.49%. For the Adaptive Thresholding technique, the results of accuracy, sensitivity, and specificity were 90.46%, 67.55%, and 91.77% respectively. The Otsu Thresholding technique was 89.32%, 92.62%, and 89.08% respectively.

The results of comparison of DRIVE dataset, it can be seen that the highest accuracy value obtained is 95.96% using Otsu Thresholding and the lowest accuracy value is 89.53% using Bradley Threshold. And the sensitivity value in Otsu thresholding is also the highest result with a value of 90.37% while Bradley Threshold gets the lowest sensitivity value with 61.97%. For the results of specificity, the ISODATA technique obtained the highest results with a value of 98.36% and the lowest specificity found in the Bradley Threshold technique with a value of 91.69%.

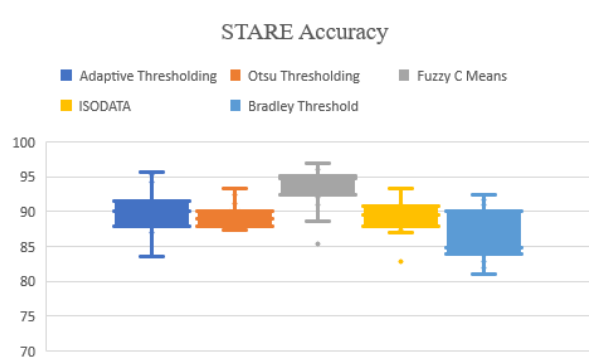


Figure 2. Graph of accuracy comparison on stare dataset

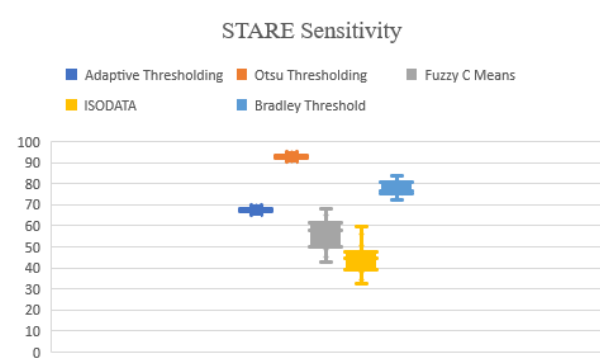


Figure 3. Graph of sensitivity comparison on stare dataset

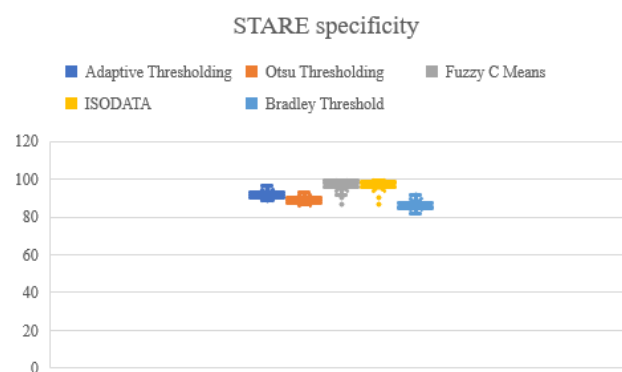


Figure 4. Graph of the specificity comparison on the stare dataset

In Figure 2. the graph of the accuracy comparison on the STARE dataset, the Fuzzy C Means Method gets the highest accuracy value of 96.95% and the lowest accuracy value is 85.32%. The Bradley Threshold method gets the highest accuracy value of 92.44% and the lowest accuracy value is 81.05%. The Adaptive Thresholding method gets the highest accuracy value of 95.70% and the lowest accuracy value is 83.53%. The Otsu Thresholding method gets the highest accuracy value of 93.24% and the lowest accuracy value is 87.33%. And the ISODATA method gets the highest accuracy value of 93.28% and the lowest accuracy value is 82.88%.

In Figure 3. the graph of the sensitivity comparison on the stare dataset, the otsu thresholding method gets the highest sensitivity value of 94.63% and the lowest sensitivity value of 90.97%. The ISODATA method gets the highest sensitivity value 59.71% and the lowest sensitivity value 32.31%. The Adaptive Thresholding method gets the highest sensitivity value of 69.50% and the lowest sensitivity value of 65.92%. The Fuzzy C Means method gets the highest sensitivity value of 67.81% and the lowest sensitivity value of 42.61%. The Bradley Threshold method gets the highest sensitivity value of 84.00% and the lowest sensitivity value of 72.53%.

In Figure 4. the graph of the comparison of the specificity of the stare dataset, the ISODATA method has the highest specificity value of 99.59% and the lowest specificity value of 86.80%. The Bradley Threshold method has the highest specificity value of 93.12% and the lowest specificity value is 81.79%. The Adaptive Threshold method got the highest specificity value of 96.43% and the lowest specificity value was 88.68%. The Fuzzy C Means method gets the highest specificity value 99.37%

and the lowest specificity value is 86.57%. The Otsu thresholding method got the highest specificity value of 93.24% and the lowest specificity value was 87.01%.

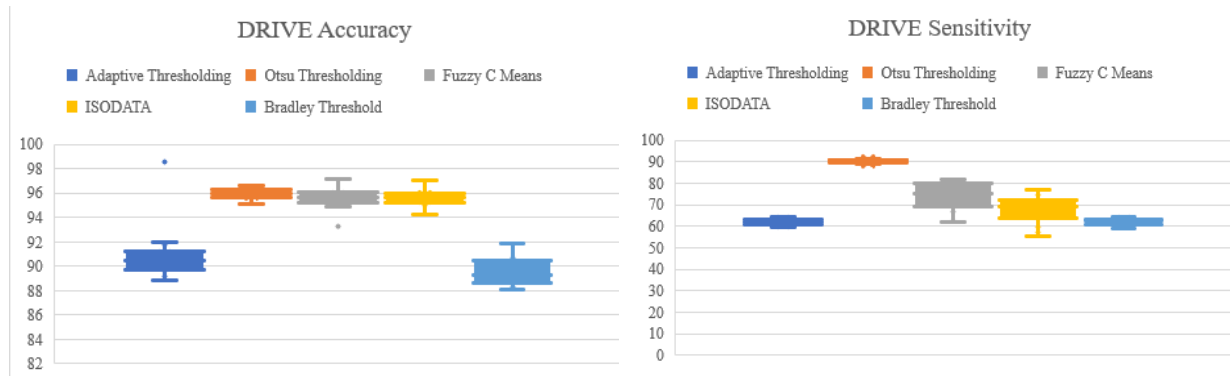


Figure 5. Graph of accuracy comparison on dataset drive

Figure 6. Graph of sensitivity comparison on dataset drive

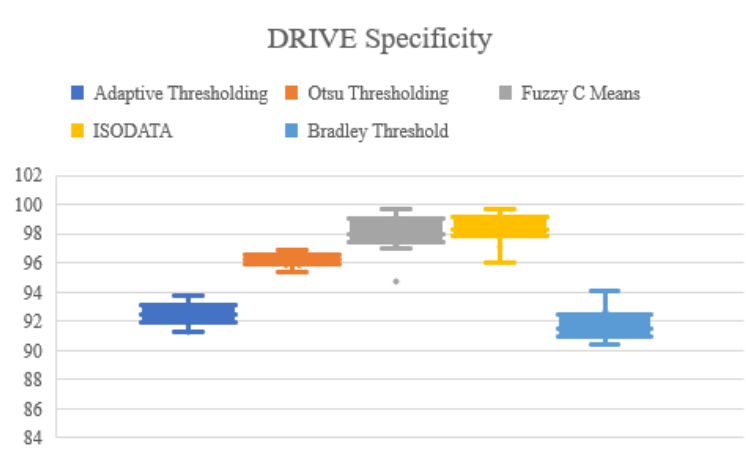



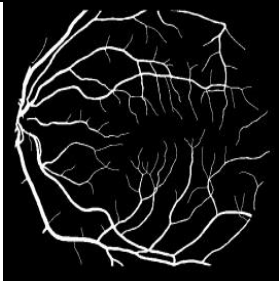

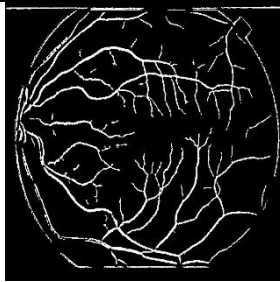



Figure 7. Graph of the specificity comparison on the dataset drive

In figure 5. Graphs of accuracy comparison on the DRIVE dataset. The Otsu Thresholding method gets the highest accuracy value of 96.64% and the lowest value is 95.11%. The Bradley Threshold method gets the highest accuracy value of 91.89% and the lowest accuracy value is 88.10%. The Adaptive Threshold method gets the highest accuracy value of 98.52% and the lowest accuracy value is 88.88%. The Fuzzy C Means method gets the highest accuracy value of 97.13% and the lowest accuracy value is 93.31%. The ISODATA method gets the highest accuracy value of 97.01% and the lowest accuracy value is 94.19%.

In Figure 6. the sensitivity comparison graph on the DRIVE dataset. The Otsu Thresholding method got the highest sensitivity value of 91.19% and the lowest sensitivity value was 89.14%. The Bradley Threshold method has the highest sensitivity value of 64.26% and the lowest sensitivity value of 58.89%. The Adaptive Thresholding method obtained the highest sensitivity value of 64.47% and the lowest sensitivity value of 59.70%. The Fuzzy C Means method gets the highest sensitivity value of 81.93% and the lowest sensitivity value of 61.84%. The ISODATA method gets the highest sensitivity value of 76.86% and the lowest sensitivity value of 55.17%.


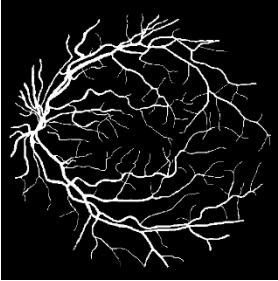

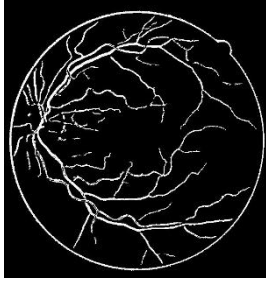
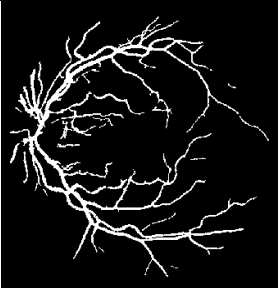
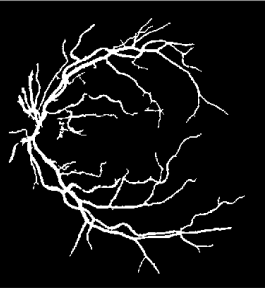

In Figure 7. graph the specificity comparison on the DRIVE dataset. The ISODATA method has the highest specificity value of 99.64% and the lowest specificity value is 96.07%. The Bradley Threshold method has the highest specificity value of 94.06% and the lowest specificity value of 90.43%. The Adaptive Thresholding method got the highest specificity value of 93.77% and the lowest specificity value was 91.29%. The Fuzzy C Means method gets the highest specificity value of 99.69% and the lowest specificity value is 94.77%. The Otsu thresholding method got the highest specificity value of 96.87% and the lowest specificity value was 95.40%.

Table 2. Results segmentation and extraction dataset of stare

 im0077.jpg			
	Ground Truth	Adaptive Thresholding	Otsu Thresholding
			
	Fuzzy C Means	ISODATA	Bradley Threshold

In Table 2, the result of the segmentation and extraction in the image dataset STARE im0077.jpg. In the Adaptive Threshold method get the results of accuracy, sensitivity, and specificity of 88.88%, 66.60%, 90.39%. The Otsu Thresholding method gets the results of accuracy, sensitivity, and specificity of 88.53%, 92.01%, 88.28%. The Fuzzy C Means method gets the results of accuracy, sensitivity, and specificity of 95.08%, 60.99%, 98.15%. The ISODATA method gets the results of accuracy, sensitivity, and specificity of 90.20%, 48.08%, 98.09%. And the Bradley Threshold method gets the accuracy, sensitivity, and specificity results of 83.80%, 75.16%, 84.90%.

Table 3. Results segmentation and extraction dataset of drive

 01_test.tif	 Ground Truth	 Adaptive Thresholding	 Otsu Thresholding
	 Fuzzy C Means	 ISODATA	 Bradley Threshold

In Table 3 is the result of the segmentation and extraction in the image dataset 01_test.tif DRIVE. In the Adaptive Threshold method get the results of accuracy, sensitivity, and specificity of 89.31%, 61.08%, 91.63%. The Otsu Thresholding method gets the results of accuracy, sensitivity, and specificity of 95.11%, 89.46%, 95.40%. The Fuzzy C Means method obtained the results of accuracy, sensitivity, and specificity of 96.24%, 76.85%, 98.51%. The ISODATA method gets the results of accuracy, sensitivity, and specificity of 96.03%, 70.35%, 98.55%. And the Bradley Threshold method gets the results of accuracy, sensitivity, and specificity of 88.46%, 59.95%, 90.90%.

In Table 2 and Table 3 is one example of the results of segmentation in each method using the STARE and DRIVE dataset. The best segmentation method among the techniques we use in this study is Otsu Thresholding, because this method is able to segment fine vessels in retinal images. In segmenting blood vessels with some of the techniques that we have done, there is still noise in some retinal images. Especially in the STARE dataset, because the images on the dataset have abnormalities such as exudates, microaneurysms, and haemorrhage.

5. Conclusion

Overall the best segmentation technique is the Otsu Thresholding method, because this technique obtains balanced results of accuracy, sensitivity, and specificity. But in this technique, the edges in some retinal images are still detected. The best accuracy value in the STARE dataset is 93.66%. The best sensitivity value in the STARE dataset is 92.62% and the best specification value in the STARE dataset is 96.85%. In the DRIVE dataset, the best accuracy value is 95.96%. The best sensitivity value is equal to 90.37% and the best specification value is 98.36%. Overall the techniques we use have been able to segment blood vessels in retinal images well.

For future research, you can add several methods that can eliminate noise in retinal images and can segment fine blood vessels for better results.

References

- [1] M. F. Aslan, M. Ceylan, and A. Durdu, "Segmentation of Retinal Blood Vessel Using Gabor Filter and Extreme Learning Machines," *2018 Int. Conf. Artif. Intell. Data Process.*, no. February 2019, pp. 1–5, 2018.
- [2] L. S. U. Ozkaya, Ş. Ozturk, B. Akdemir, "An Efficient Retinal Blood Vessel Segmentation using Morphological Operations," in *International Symposium on Multidisciplinary Studies and Innovative Technologies (ISMSIT)*, 2018.
- [3] J. Dash and N. Bhoi, "Retinal blood vessel segmentation using Otsu thresholding with principal component analysis," *Proc. 2nd Int. Conf. Inven. Syst. Control. ICISC 2018*, no. Icisc, pp. 933–937, 2018.
- [4] S. Kaur and D. K. S. Mann, "Optimized Retinal Blood Vessel Segmentation Technique For Detection Of Diabetic Retinopathy," *J. Adv. Res. Comput. Sci.*, vol. 8, no. 0976, pp. 508–512, 2017.
- [5] & Y. R. Zhun Fan, Jiewei Lu, "Automated Blood Vessel Segmentation of Fundus Images Using Region Features of Vessels," *2016 IEEE Symp. Ser. Comput. Intell.*, 2016.
- [6] F. Farokhian, C. Yang, H. Demirel, S. Wu, and I. Beheshti, "Automatic parameters selection of Gabor filters with the imperialism competitive algorithm with application to retinal vessel segmentation," *Integr. Med. Res.*, vol. 37, no. 1, pp. 246–254, 2017.
- [7] U. Ozkaya, B. Akdemir, and L. Seyfi, "An Efficient Retinal Blood Vessel Segmentation using Morphological Operations," *2018 2nd International Symposium on Multidisciplinary Studies and Innovative Technologies (ISMSIT)*, 2018, pp. 1-7.
- [8] L. Câmara, G. L. B. Ramalho, J. F. S. Rocha, and R. M. S. Veras, "An unsupervised coarse-to-fine algorithm for blood vessel segmentation in fundus images," *Expert Syst. Appl.*, vol. 78, no. February, pp. 182–192, 2017.
- [9] A. Biran, P. S. Bidari, A. Almazroa, and K. Raahemifar, "Blood Vessels Extraction from Retinal Images Using Combined 2D Gabor Wavelet Transform with Local Entropy Thresholding and Alternative Sequential Filter," *IEEE Can. Conf. ECE*, pp. 1–5, 2016.
- [10] L. C. Rodrigues and M. Marengoni, "Segmentation of optic disc and blood vessels in retinal images using wavelets, mathematical morphology and Hessian-based multi-scale filtering," *Biomed. Signal Process. Control*, vol. 36, pp. 39–49, 2017.
- [11] H. A. Nugroho, R. A. Aras, T. Lestari, and I. Ardiyanto, "Retinal Vessel Segmentation Based on Frangi Filter and Morphological Reconstruction," in *The 2017 International Conference on Control, Electronics, Renewable Energy and Communications (ICCEREC)*, 2017, no. 1, pp. 181–184.
- [12] C. Zhu *et al.*, "Retinal vessel segmentation in colour fundus images using Extreme Learning Machine," *Comput. Med. Imaging Graph.*, vol. 55, pp. 68–77, 2017.
- [13] M. Zardadi, N. Mehrshad, and S. M. Razavi, "Unsupervised Segmentation of Retinal Blood Vessels Using the Human Visual System Line Detection Model," *J. Inf. Syst. Telecommun.*, vol. 4, no. 2, pp. 125–133, 2016.

- [14] M. Baj, P. Sekuli, S. Djukanovi, T. Popovi, and S. Member, "Retinal blood vessels segmentation using ant colony optimization," *Symp. Neural Networks Appl.*, pp. 22–24, 2016.
- [15] A. Subudhi, "Blood vessel extraction of diabetic retinopathy using optimized enhanced images and matched filter optimized enhanced images and matched filter," *J. Med. Imaging*, vol. 3, no. 4, 2017.
- [16] S. Ayaz, A. Shah, T. B. Tang, I. Faye, and A. Laude, "Blood vessel segmentation in color fundus images based on regional and Hessian features," *Graefe's Arch. Clin. Exp. Ophthalmol.*, vol. 255, no. 8, pp. 1525–1533, 2017.
- [17] N. Dey *et al.*, "FCM Based Blood Vessel Segmentation Method for Retinal Images," *Int. J. Comput. Sci. Netw.*, vol. 1, no. 3, pp. 1–5, 2012.
- [18] R. Kamble, "Automatic Blood Vessel Extraction Technique Using Phase Stretch Transform In Retinal Images." *2016 International Conference on Signal and Information Processing (ICoNSIP), 2016*, pp. 1-5.
- [19] K. Mehta and M. T. S. Cse, "An Enhanced Segmentation Technique for Blood Vessel in Retinal Images," *Int. J. Comput. Appl.*, vol. 150, no. 6, pp. 9–15, 2016.
- [20] O. MARQUES, *Practical image and video processing using matlab* ®. John Wiley & Sons, Inc., Hoboken, New Jersey, 2011.
- [21] V. K. and M. G. A. Hoover, "Locating Blood Vessels in Retinal Images by Piece-wise Threhsold Probing of a Matched Filter Response," *IEEE Trans. Med. Imaging*, vol. 19 no, pp. 203–210, 2003.
- [22] J. J. Shi, M. Li, S. Han, and J. Shi, "An enhanced ISODATA algorithm for recognizing multiple electric appliances from the aggregated power consumption dataset," *Energy Build.*, vol. 140, no. October, pp. 305–316, 2017.
- [23] J. Dash, "Retinal Blood Vessels Extraction from Fundus Images Using an Automated Method," *2018 4th Int. Conf. Recent Adv. Inf. Technol.*, pp. 1–5, 2018.
- [24] D. Oliva, E. Cuevas, G. Pajares, D. Zaldivar, and M. Perez-Cisneros, "Multilevel thresholding segmentation based on harmony search optimization," *J. Appl. Math.*, vol. 2013, pp. 1-24, 2013.